

DECEMBER 31 2003

## Sound transmission characteristics of Tee-junctions and the associated length corrections ✓

S. K. Tang



*J. Acoust. Soc. Am.* 115, 218–227 (2004)

<https://doi.org/10.1121/1.1631830>



### Articles You May Be Interested In

On low frequency sound transmission loss of double sidebranches: A comparison between theory and experiment

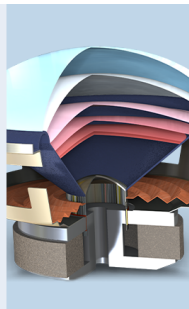
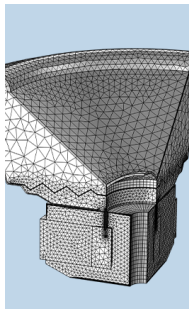
*J Acoust Soc Am* (May 2003)

Narrow sidebranch arrays for low frequency duct noise control

*J. Acoust. Soc. Am.* (November 2012)

Narrow sidebranches for duct silencing

*J Acoust Soc Am* (April 2012)



COMSOL

## Find your best idea

with multiphysics modeling  
and simulation apps

« LEARN MORE

# Sound transmission characteristics of Tee-junctions and the associated length corrections

S. K. Tang<sup>a)</sup>

*Department of Building Services Engineering, The Hong Kong Polytechnic University, Hong Kong, China*

(Received 30 March 2003; revised 22 August 2003; accepted 17 October 2003)

The sound transmission characteristics of a Tee-junction formed by a sidebranch and an infinitely long duct are investigated numerically using the finite element method. The associated corrections of the branch length and the upstream duct length are also discussed in detail. The types of branch resonance that result in strong or weak sound transmission across the junction are determined and their effects on the length corrections examined. Results suggest that the type of sidebranch, the branch width, the branch length, and the order and the form of the resonance affect more significantly the length corrections of the duct section. The excitation of nonplanar higher branch modes gives rise to rapid increase in the duct length corrections and also results in lower sound transmission. © 2004 Acoustical Society of America. [DOI: 10.1121/1.1631830]

PACS numbers: 43.50.Gf, 43.20.Mv [DKW]

Pages: 218–227

## I. INTRODUCTION

Sidebranches are very commonly found in modern buildings with centralized air conditioning systems. They help the distribution of treated air from the air handling units into the occupied zones inside a building. It has been shown that a sidebranch offers a change in the acoustic impedance along the main duct and thus results in sound transmission loss.<sup>1</sup> A formula for the prediction of this sound transmission loss can also be found in textbooks (for instance, Ref. 2). However, this formula is accurate only at very low frequency. Also, such a change in acoustic impedance alters the resonant characteristics along the main duct section upstream of the sidebranch. A length correction for this section is expected.

The issue of the end correction for plane wave motion for duct openings with and without flanges is well known.<sup>1</sup> This correction affects the resonance frequencies of the duct. The larger the opening, the greater will be this correction. However, the corresponding correction due to diffraction and/or scattering at a discontinuity internal to a duct is rarely discussed. The theoretical deduction of Miles<sup>3</sup> using the conformal mapping technique works only at very low frequency. Bruggeman<sup>4</sup> assumed plane waves inside the sidebranches and the main duct except in a limited region inside the junction. This assumption is valid only at low frequency. Neither the results of Bruggeman<sup>4</sup> nor the more recent results from Redmore and Mulholland<sup>5</sup> enable an estimation of such a correction. Knowledge of this correction in a reasonable frequency range will enable a better prediction of the sound transmission loss and provide clues for the physical explanation of acoustical properties of multiconnected duct elements along a duct.

Recently, the experimental results of the author on sound transmission across a single sidebranch revealed the presence of two main branch impedance types.<sup>6</sup> The first one is a high-pass filter type. This corresponds to the case of an infi-

nitely long branch or zero branch length opening. The second one involves the longitudinal resonance inside the branch and is of the band-stop filter type. It has also been shown that a specific correction in the separation between two identical sidebranches is required to explain the measured sound power transmission loss. However, an exact explanation has not been sought, as the knowledge of the length correction due to diffraction at the branch entrances is currently unknown.

In the present study, the sound field and the acoustic length correction due to the presence of a Tee-junction in a duct are investigated using the method of finite elements. This method can allow for a much higher degree of nonuniformity in pressure/velocity distribution inside the sidebranches than that of Bruggeman.<sup>4</sup> The frequency concerned is up to the first eigenfrequency of the duct, so that plane wave propagation inside the duct at distances sufficiently far away from the branch is guaranteed. It is hoped that the present results can provide a stepping stone for investigation of the acoustical properties of duct element systems with more complicated connections.

## II. COMPUTATIONAL MODEL AND THEORY

Figure 1 illustrates the schematic of the sidebranch and duct system (Tee-junction) and the nomenclature adopted. All length scales are normalized by the duct width  $d$ . The branch length  $l$  and the branch width  $w$  are allowed to vary relative to  $d$ . As only plane incident waves will be considered in the present study, the sound field dealt with here is uniform in the direction normal to the  $x$ - $y$  plane. The finite element computations for solving the standard wave equation

$$\nabla^2 p + k^2 p = 0, \quad (1)$$

where  $p$  and  $k$  denote the acoustic pressure and the wave number of the sound, respectively, are implemented using the software MATLAB. The computation domain starts at  $x/d = -5$  and ends at  $x/d = w/d + 6$ . These locations are far enough for all evanescent waves scattered and/or diffracted by the sidebranch to decay completely. At  $x/d = -5$ , the

<sup>a)</sup>Electronic mail: besktang@polyu.edu.hk

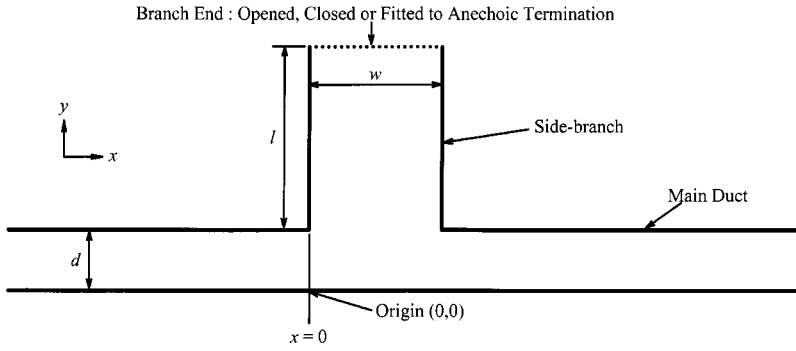


FIG. 1. Schematic of the Tee-junction and nomenclature adopted.

sound field is made up of a forward and a backward propagating plane wave, while that at  $x/d = w/d + 6$  consists of a forward propagating plane wave only. The acoustic pressures in the foregoing discussion are normalized by the incident wave magnitude. As in Ref. 7, the corresponding boundary conditions are

$$\frac{\partial p}{\partial n} + ikp = \begin{cases} 2ik & \text{at } x/d = -5, \\ 0 & \text{at } x/d = w/d + 6, \end{cases} \quad (2)$$

where  $n$  represents the outward normal direction of a boundary. The boundary conditions on boundaries other than the branch exit follow that of a rigid wall of vanishing normal acoustic particle velocity. The sound frequency is kept below the first higher-mode eigenfrequency of the main duct.

The boundary condition at the branch exit substantially affects the type of filtering action the sidebranch offers to the wave propagating along the main duct. In the present study, three types of branch endings will be considered. The first type refers to an infinitely long branch, which does not produce sound reflection back into the main duct. The impedance-matched anechoic termination of Tang and Lau<sup>7</sup> is adopted at  $y/d = 6$ ,  $0 < x < w$ , instead of the plane wave condition in order to attenuate any higher branch modes and evanescent waves that may have been created in the Tee-junction. However, one should note that the branch impedance in this case does not depend on the branch length  $l$ . Such a branch produces a high-pass filtering action until the cuton of the first higher mode in the branch or in the main duct. The second type is an opened branch. For simplicity, the condition of  $p = 0$  at  $y = l + d$ ,  $0 < x < w$  is adopted. In this case,  $l$  includes the open-end correction due to exit radiation impedance.<sup>1</sup> A high-pass filtering action is created before resonance occurs. The last type is the closed branch.<sup>8</sup> The boundary condition at  $y = l + d$ ,  $0 < x < w$  is  $\partial p / \partial y = 0$ . This branch produces low-pass filtering action up to the first longitudinal branch resonance frequency. These branch end conditions cover those categorized by Tang and Li.<sup>6</sup>

Although one expects the sound field to be nonplanar in the vicinity of the Tee-junction, the waves far away from the junction are still planar. The acoustic length correction for the upstream duct section due to the Tee-junction,  $\epsilon$ , is determined by the wave number or frequency at which the input impedance  $Z_{in}$  to the system has vanishing reactance and its magnitude reaches a local minimum in the frequency variation.<sup>1</sup> The input impedance can be estimated once the acoustic pressure field at the system inlet ( $x/d = -5$ ) and its gradient are obtained:

$$\frac{Z_{in}}{\rho c S} = -i \frac{k p_{x/d=-5}}{\partial p / \partial x|_{x/d=-5}}, \quad (3)$$

where  $\rho$  is the ambient air density,  $c$  the speed of sound, and  $S$  the cross-sectional area of the main duct, which is not important in the present study. The wave number  $k_j$  at which the  $j$ th order resonance occurs can then be found. They are related to the acoustical length correction  $\epsilon_j$  by

$$k_j = \frac{j\pi}{L + \epsilon_j} \Rightarrow \epsilon_j = \frac{j\pi}{k_j} - L, \quad (4)$$

where  $L$  is the distance from the branch at which the duct system is being driven and is equal to  $5d$  in the present study.  $L$  does not affect the length corrections.<sup>1</sup> The frequencies of longitudinal branch resonances determined by the computation are used to estimate the length corrections for the branches in a similar manner with  $L$  replaced by  $l$ . Since the computational results for acoustic pressure are normalized by the incident sound wave magnitude, the squared strength of the transmitted sound wave,  $|p_{x/d=w/d+6}|^2$ , equals the sound power transmission coefficient, which is denoted by  $\tau$  in the foregoing discussion.

The maximum branch width included here is  $1.8d$ . This is already outside the practical dimension, which is usually  $w/d \leq 1$ . However, the range of  $1 < w/d \leq 1.8$  is included for the sake of completeness. The branch length investigated is up to  $5d$ .

### III. RESULTS AND DISCUSSION

#### A. Infinitely long branches

The acoustical properties of infinitely long branches do not depend on the branch length  $l$ . However, it would be better to have a length not less than  $6d$  so that the computational requirement of the numerical anechoic termination is less demanding. No standing wave is set up in the branches throughout the numerical experiment.

Figure 2 shows the variation of sound power transmission along the main duct with wave number (frequency) before the first eigenfrequency of the duct. The importance of the branch width  $w$  is manifested. For  $w/d < 1$ , the branch is a high-pass filter, and the sound transmission becomes more and more effective as  $kd$  approaches  $\pi$ . For  $w/d > 1$ , the first higher branch mode is excited before that of the main duct. Again  $\tau$  increases with frequency, but this time with a faster rate than that for  $w/d < 1$ , and reaches a local maximum at or very close to the eigenfrequency of the branch. After that,  $\tau$

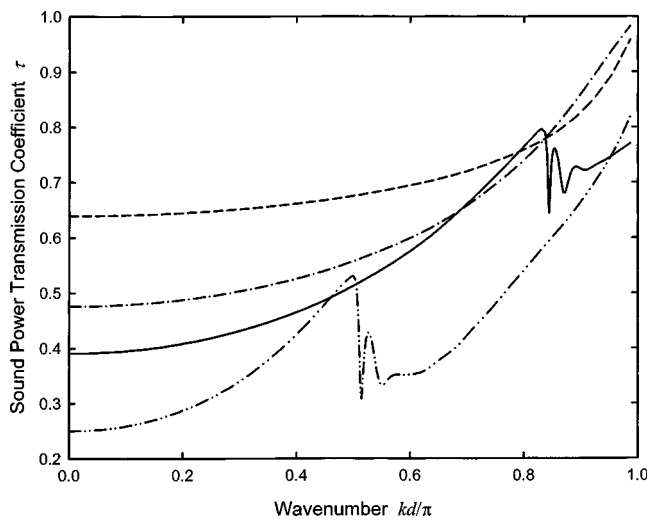


FIG. 2. Sound power transmission across an infinitely long sidebranch along the main duct. —:  $w/d=0.5$ ; ---:  $w/d=0.9$ ; —·—:  $w/d=1.2$ ; ···:  $w/d=2$ .

fluctuates chaotically before it resumes its increasing trend as  $kd$  approaches the upper limit of the present study. This observation appears consistent with the experimental observation of Redmore and Mulholland,<sup>5</sup> which shows that the sound power transmission loss along the main duct around the first higher branch mode eigenfrequency appears at frequency slightly higher than this frequency. This will be discussed further later. For  $w/d > 1$ , the maximum  $\tau$  before the cuton of the first branch asymmetric higher mode decreases as  $w$  increases. At very low frequency,  $kd \rightarrow 0$ , and one can observe that

$$\tau = \left( \frac{d}{d + 0.5w} \right)^2, \quad (5)$$

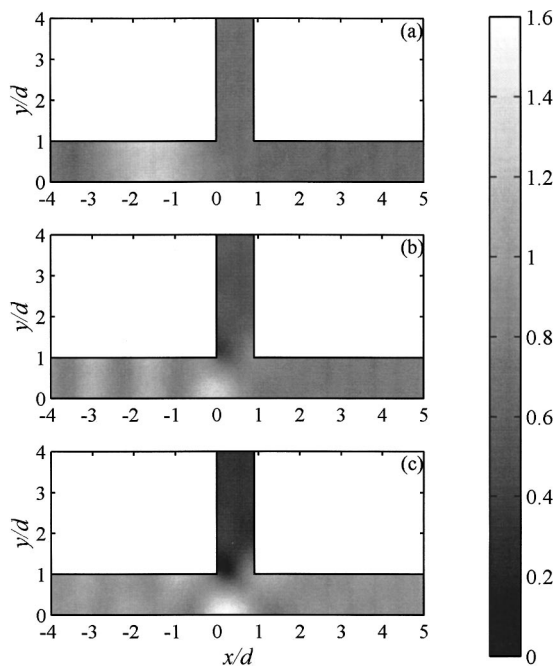


FIG. 3. Sound field around Tee-junction of an infinitely long sidebranch of  $w/d=0.9$ .  $kd =$  (a)  $0.254\pi$ , (b)  $0.729\pi$ , and (c)  $0.923\pi$ .

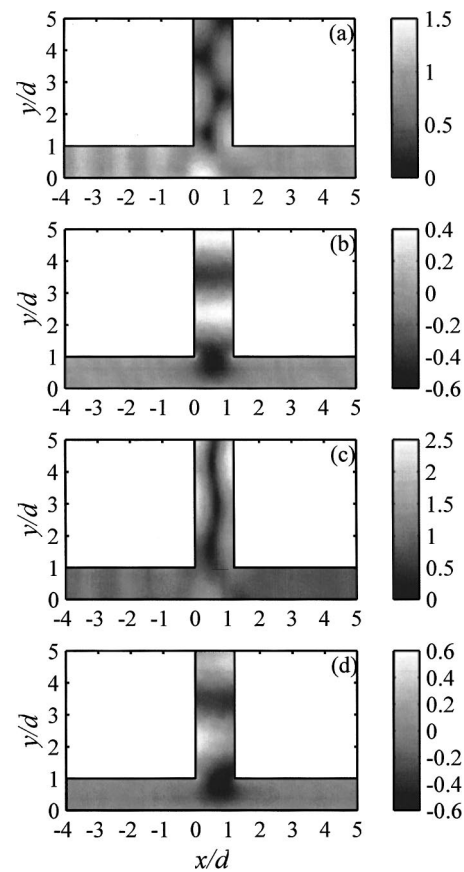


FIG. 4. Sound field around Tee-junction of an infinitely long sidebranch of  $w/d=1.2$ . (a)  $kd=0.833\pi$ , pressure magnitude; (b)  $kd=0.833\pi$ , upward particle velocity; (c)  $kd=0.844\pi$ , pressure magnitude; (d)  $kd=0.844\pi$ , upward particle velocity.

which agrees with the prediction of the low-frequency plane wave theory<sup>1</sup> regardless the ratio  $w/d$ .

Figure 3 illustrates some sound fields around the Tee-junction for  $w/d=0.9$ . At low frequency, the sound field close to the entry of the Tee-junction is planar, while a strong standing wave is observed in the upstream duct, suggesting that a strong reflection exists [Fig. 3(a)]. As the frequency increases, greater sound energy is accumulated inside the junction [Fig. 3(b)] due to the higher diffraction effectiveness at higher frequency.<sup>9</sup> This produces stronger excitation in the plane wave propagation into the downstream duct and thus reduces the sound power transmission loss. At frequencies close to the first higher eigenfrequency of the duct, some nonplanar sound waves can be found within and at some distances downstream of the junction because of the acoustic scattering and diffraction as expected [Fig. 3(c)]. These evanescent waves decay quickly inside the duct and the branch.

Sound fields for  $w/d > 1$  are more complicated, although those at frequencies before the first higher eigenfrequency of the branch resemble very much those shown in Fig. 3. The characteristics of the sound field development for all  $w$  larger than  $d$  are essentially the same and thus only the case of  $w/d=1.2$  will be illustrated. As the sound frequency approaches the first eigenfrequency of the branch with  $w/d=1.2$  ( $kd=\pi/1.2 \sim 2.62$ ), one can observe that the sound energy gradually fills up the inlet of the branch [Fig. 4(a)] and the distribution of acoustic velocity (upward)



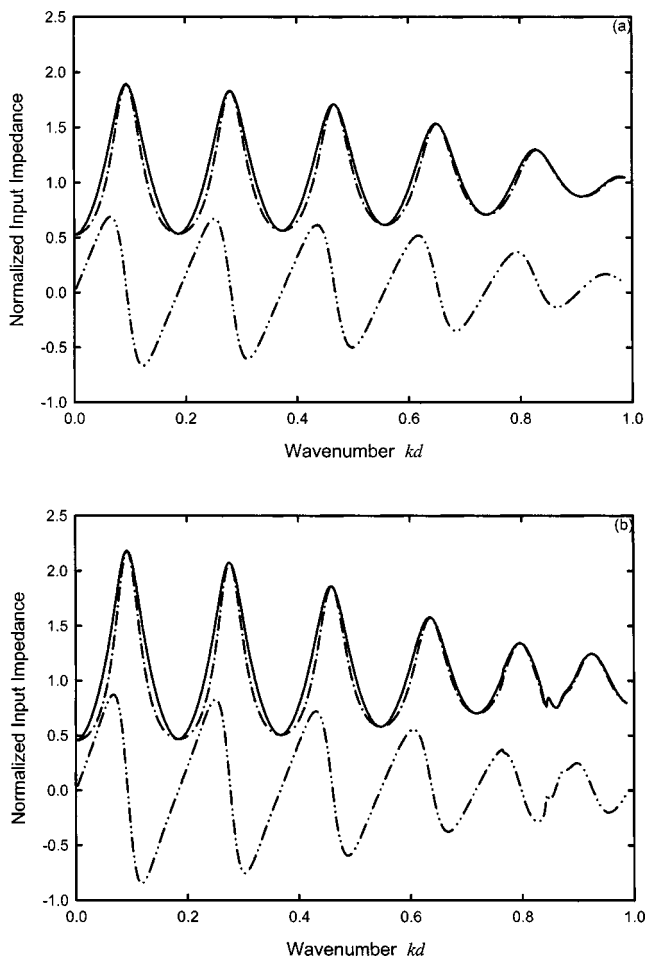


FIG. 5. Frequency variation of input impedance with an infinitely long sidebranch.  $w/d =$  (a) 0.9; (b) 1.2. —: Impedance magnitude; - - -: resistance; - · - · -: reactance.

inlet at frequency very close to the mentioned branch eigenfrequency is symmetrical about the branch axis [Fig. 4(b)]. Therefore, the first higher branch mode, which is asymmetric, is not properly excited even when the frequency reaches the mode eigenfrequency. At higher frequency, the wavelength of the sound becomes smaller than  $2w$ . Strong resonance of the higher branch mode can then be observed [Fig. 4(c)]. This strong resonance takes away a considerable amount of acoustic energy, resulting in a drop of the sound power transmission (Fig. 2). The corresponding upward particle velocity field, shown in Fig. 4(d), illustrates the asymmetric excitation at the branch inlet around this critical frequency.

Figures 5(a) and 5(b) illustrate the frequency variations of the normalized input impedance  $Z_{in}/\rho cS$  for  $w/d = 0.9$  and 1.2, respectively. The local minima of the impedance magnitude occur at frequencies of vanishing reactance for both  $w$ . At very low frequency, that is,  $kd \rightarrow 0$ , the present results suggest that  $Z_{in}$  is real and conforms to the low-frequency theory<sup>1</sup> prediction that

$$Z_{in} = \rho cS \frac{d}{w+d}. \quad (6)$$

Figure 5 also shows that the reactance tends to converge toward zero and the resistance toward unity as the frequency

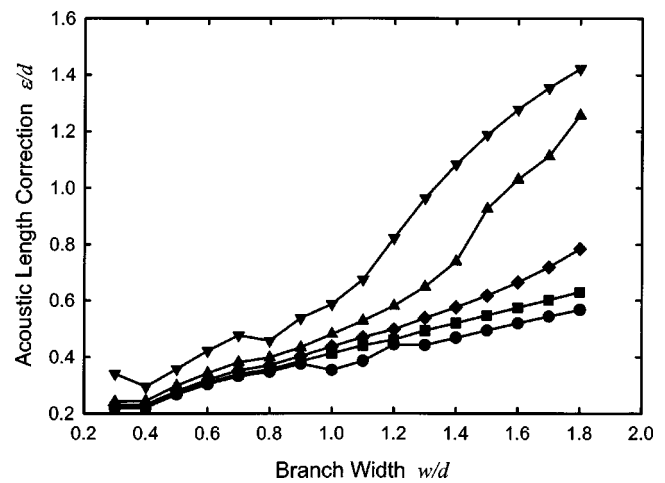


FIG. 6. Acoustic length corrections in the presence of an infinitely long sidebranch. ●: first order; ■: second order; ◆: third order; ▲: fourth order; ▼: fifth order.

increases toward the eigenfrequency of the first asymmetric higher duct mode. These features of  $Z_{in}$  are observed for other  $w/d$ . The very high-power transmission at frequency close to the first duct mode eigenfrequency, as illustrated in Fig. 2, is accompanied by a large reduction in the reflected wave energy as the resistance to wave propagation becomes weak. The situation becomes similar to that of an infinitely long duct without the sidebranch and thus  $Z_{in} \rightarrow \rho cS$ . This is consistent with the computed results even with the presence of evanescent waves in the vicinity of the Tee-junction. The propagation of higher branch modes does not offset the general trend of  $Z_{in}$  variation, except for the minor smooth but relatively rapid fluctuations close to the first branch mode eigenfrequency [Fig. 5(b)].

Figure 6 shows the variation of the acoustic length corrections for the first five order resonances of the main duct with wave number. Unlike the case for the open-ended tube, these corrections increase with frequency as diffraction and wave scattering are in general more efficient at higher frequency.<sup>9</sup> They also increase with  $w$  in general, although there are occasional irregularities in the increasing trend. Such irregularities are probably due to the very frequency and geometry dependent diffraction, which leads to nonuniform distribution of acoustic pressure and air particle velocities near the branch entrance. For small  $w$ , the first four order length corrections are very similar. The difference increases with  $w$ , and this increase accelerates when the higher branch mode starts to propagate. The fifth order resonance at  $w/d = 1.2$  occurs after this higher-mode cuton, while at  $w/d = 1.5$ , the fourth one occurs. Those lower-order resonances occur before such a cuton in the present range of  $w/d$ . The propagation of higher branch modes enhances the spreading of acoustical energy across the Tee-junction. It is also noted that the first three order length corrections and those of the other two orders before the higher-mode cuton increase slowly with  $w$ , and the ratio  $\epsilon/w$  actually drops as  $w/d$  increases (not shown here).

## B. Opened branches

Standing waves can be found in the branches in this case due to open-end reflection. Two types of resonance, namely,

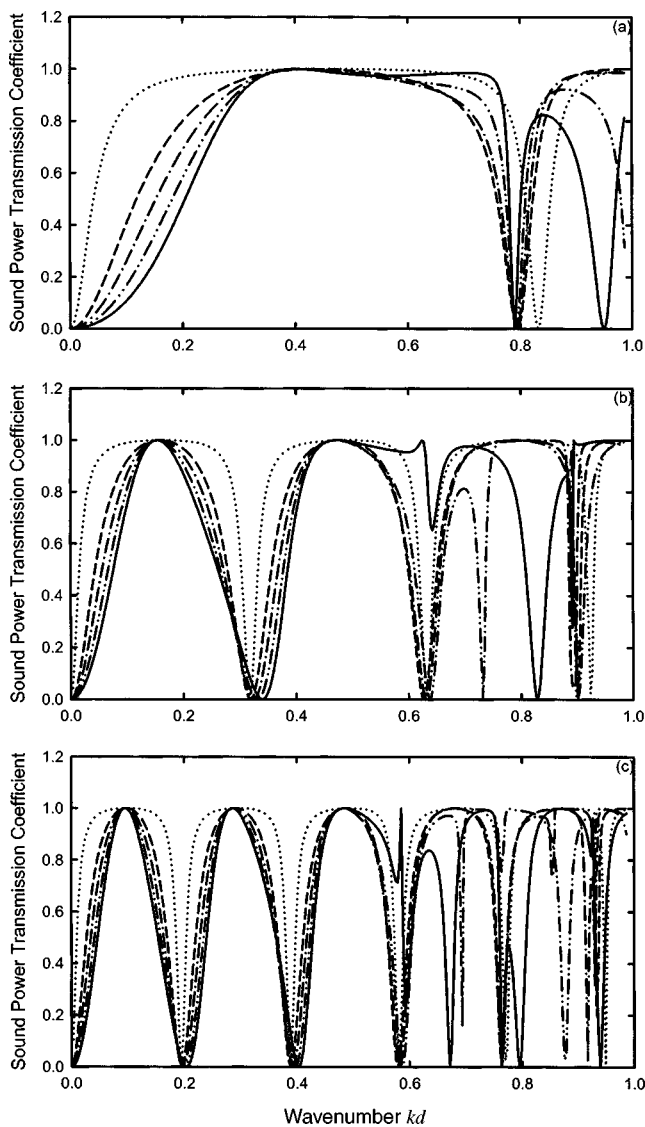


FIG. 7. Sound power transmission across open branches.  $l/d =$  (a) 1; (b) 3; (c) 5.  $\cdots$ :  $w/d = 0.3$ ;  $---$ :  $w/d = 0.9$ ;  $- \cdot - \cdot -$ :  $w/d = 1.2$ ;  $- \cdot - \cdot -$ :  $w/d = 1.5$ ;  $---$ :  $w/d = 1.8$ .

the “both ends opened” and “one end closed one end opened,” can be defined according to the wave patterns inside the sidebranches.<sup>1</sup> The former refers to the case where low-pressure regions are found at the two ends of the branch. The latter denotes the situation where the high-pressure regions are established at the duct wall opposite the branch.

The sound power transmission coefficients shown in Figs. 7(a) (b), and (c) suggest that these branches are high-pass filters at low frequency. However, one can see from the same figures that the branch length  $l$  this time has significant effects on the sound transmission. For short branch length, for instance at  $l/d = 1$ , one can find more broadband high-pass action at reduced branch width [Fig. 7(a)]. Also, apart from the case of vanishing  $kd$ , there is only one frequency at which no sound can go across the branch for  $w/d < 1$ . This vanishing sound transmission occurs twice for  $w/d > 1.2$  at  $kd < \pi$ . The frequency of the first vanishing  $\tau$  decreases as  $w$  increases and the rate of decrease decreases with increasing  $w$ . This is mainly due to a “both-end-opened” type of longi-

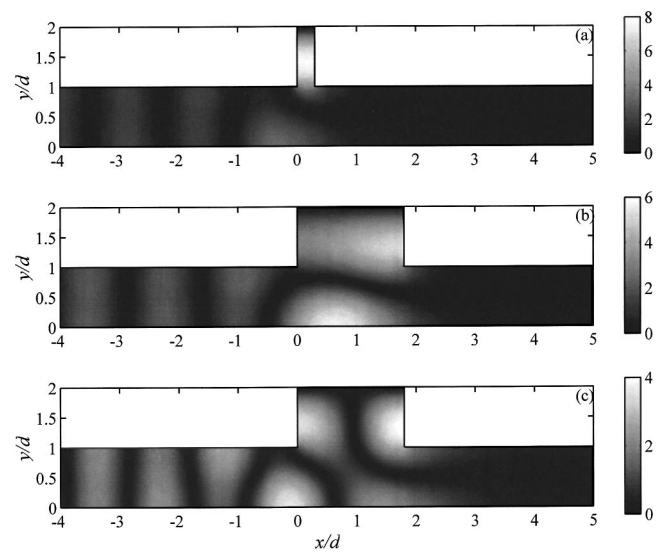


FIG. 8. Sound fields at frequencies of vanishing sound transmission for open branch cases. (a)  $kd = 0.831\pi$ ,  $w/d = 0.3$ ; (b)  $kd = 0.789\pi$ ,  $w/d = 1.8$ ; (c)  $kd = 0.949\pi$ ,  $w/d = 1.8$ ,  $l/d = 1$ .

tudinal branch resonance as shown in Fig. 8(a) (low pressure at the two ends of the branch). This appears consistent with the experimental results of Tang and Li.<sup>6</sup> However, as  $w$  increases, high sound energy accumulation inside the Tee-junction especially at  $y = 0$  is found at  $w/d = 1.8$  under the “both-end-opened” branch resonance [Fig. 8(b)]. The second vanishing  $\tau$  is due to the resonance of the first asymmetric opened branch mode [Fig. 8(c)].

The increase in the branch length  $l$  results in more occurrence of branch mode resonances and thus more frequencies of vanishing sound transmission [Figs. 7(b) and (c)]. For  $l/d = 3$ , the vanishing  $\tau$  observed at  $kd \sim 0.32\pi$  and  $0.64\pi$  are due to the type of planar longitudinal branch resonance illustrated in Figs. 8(a) and (b). However, the nodal and antinodal planes become more inclined at large  $w$  [Fig. 9(a)] and at  $w/d = 1.8$ , and this resonance cannot take place because of the excitation of the first asymmetric standing branch mode [Fig. 9(b)]. Such coexcitation of the axial and asymmetric branch modes results in a vanishing pressure region at the entry of the branch. The effective branch length is greatly reduced, increasing the sound transmission inside the main duct and thus the rise in sound transmission at the corresponding frequency observed in Fig. 7(b). The vanishing  $\tau$  for  $w/d > 1$  at  $kd > 0.7\pi$  is due to the excitation of higher-standing branch modes. This pattern repeats as  $kd$  approaches  $\pi$ . The situations for  $l/d = 5$  are the same except that the variation of  $\tau$  with frequency is more rapid. Thus, they are not discussed further. The observed high sound transmission before the excitation of higher-branch mode resonance for all  $w$  and  $l$  is due to a “one-end-closed-one-end-opened” type branch resonance<sup>1</sup> with high pressure buildup around the entry of the branch. A typical example of such a sound field is given in Fig. 9(c). This is consistent with the experimental observation of Tang and Li.<sup>6</sup>

Two length corrections are involved in this opened-branch case. One is the acoustic length correction of the main duct section upstream of the sidebranch, and the other that of the sidebranch. Figure 10(a) shows three examples of

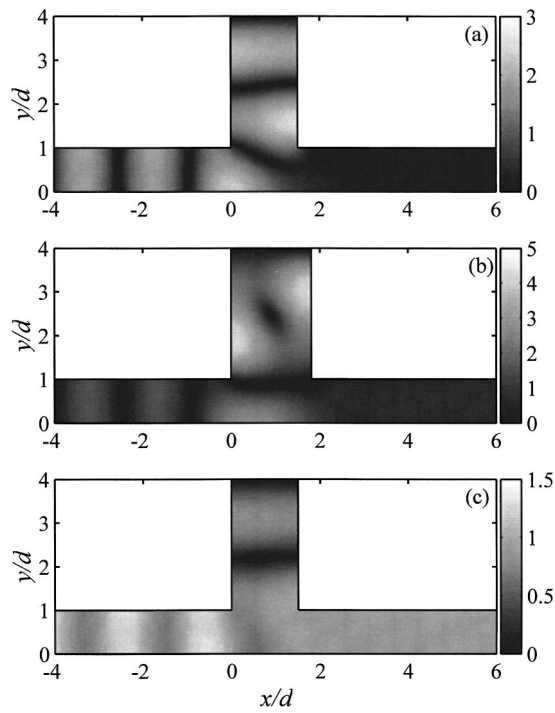


FIG. 9. Some examples of resonance inside opened sidebranch with  $l/d = 3$ . (a)  $kd = 0.630\pi$ ,  $w/d = 1.5$ ; (b)  $kd = 0.643\pi$ ,  $w/d = 1.8$ ; (c)  $kd = 0.551\pi$ ,  $w/d = 1.5$ .

the sidebranch impedance  $Z_b$  calculated using the formula in Ref. 1. The pattern of impedance variation of the  $l/d = 1$ ,  $w/d = 0.3$  case appears to be very similar to that of an open-end tube.<sup>1</sup> The situations with  $l/d = 3$ ,  $w/d = 1.3$  and  $l/d = 5$ ,  $w/d = 1.8$  are similar, except that there are a number of higher-branch standing wave modes being excited as discussed before. The weak impedance is due to a “both-end-opened” type branch resonance discussed before. The cases of high resistance (branch impedance magnitude as well) are due to the “one-end-closed-one-end-opened” branch resonance [Fig. 9(c)]. The corresponding input impedance  $Z_{in}$  is shown in Fig. 10(b). One can observe similar frequency dependence as for  $Z_b$  at low frequencies only.  $Z_{in}$  depends very much on the impedance produced by the branch, such that the resonance does not occur so regularly as in the case of infinitely long branches (Fig. 5). There are lots of vanishing reactance cases (not shown here), but only those associated with a weak impedance magnitude and a relatively weak total acoustic pressure at the inlet ( $x/d = -5$ ) indicate the occurrence of resonance. One should also note that  $Z_{in}$  depends on  $L$ , but the corrections do not.

The branch length corrections of the initial few branch resonance are summarized in Fig. 11(a). Those related to frequencies where higher branch modes are excited are excluded as the formula of Ref. 1 may not apply directly to such situation. It is noticed that for the high-sound-transmission cases (large branch resistance), the corrections are negative and do not vary much with branch length and the order of the resonance. For the case of vanishing sound transmission, the corrections are positive. They decrease as branch length increases, but are reduced at increased resonance order.

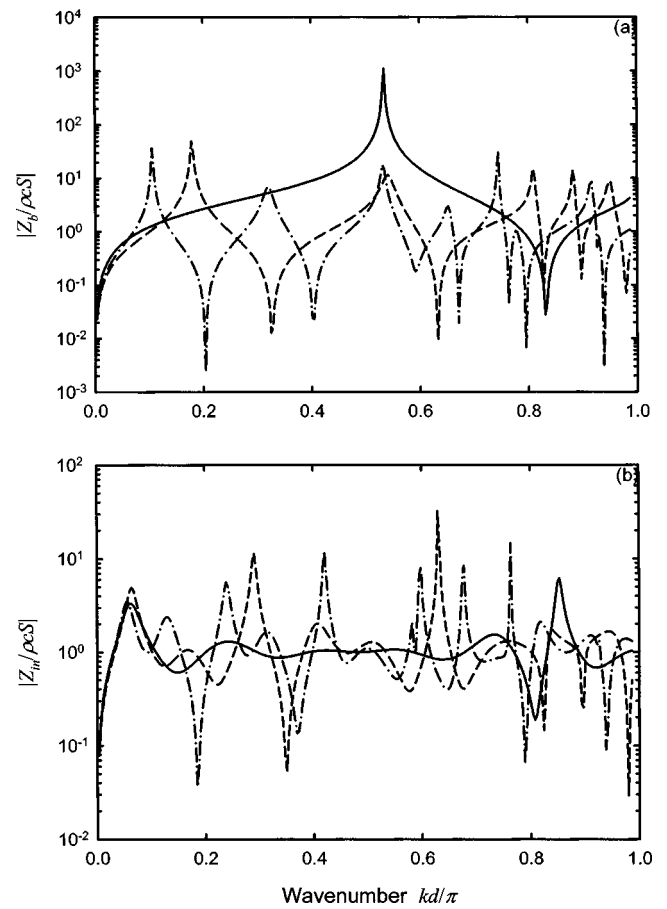


FIG. 10. Variation of mechanical impedance magnitudes with wave number for open-branch cases. (a) Sidebranch; (b) input impedance of main duct. —:  $l/d = 1$ ,  $w/d = 0.3$ ; — —:  $l/d = 3$ ,  $w/d = 1.3$ ; — · — · —:  $l/d = 5$ ,  $w/d = 1.8$ .

The acoustic length correction in the main duct does not show a very well defined trend of variation with branch length, branch width, or the order of resonance [Fig. 11(b)], but it is certain that the branch resonance plays an important role in it. For  $l/d = 1$ ,  $\epsilon_1$  decreases with increasing  $w$ , while the other corrections show the opposite trend. The resonance in the main duct in this case, especially the first and second ones, does not depend very much on the branch resonance as the first important branch resonance which results in serious reflection is located at  $kd$  near to  $\pi$ . The weak reflection, especially for short  $w$  [Fig. 10(b)], allows easy passage of sound across the branch and thus the large length correction observed. As the order of resonance increases, the duct section upstream of the branch resonates with a shorter wavelength and the correction increases with  $w$ , but decreases as the order of resonance increases. Only four duct resonance are observed at  $kd < \pi$  for  $l/d = 1$ .

The situation with  $l/d = 3$  appears very different from that with  $l/d = 1$ . The first branch resonance causing vanishing sound transmission takes place at  $kd \sim 0.33\pi$ , the second one being at  $kd \sim 0.67\pi$ . The strong reflection around these resonance frequencies gives rise to duct section resonance. The first two appear around  $kd \sim 0.3\pi$  and the third and fourth orders around  $kd \sim 0.6\pi$  [Fig. 10(b)]. The first and third duct resonances are due to the “both-end-opened” branch resonance, while the other two are produced by the

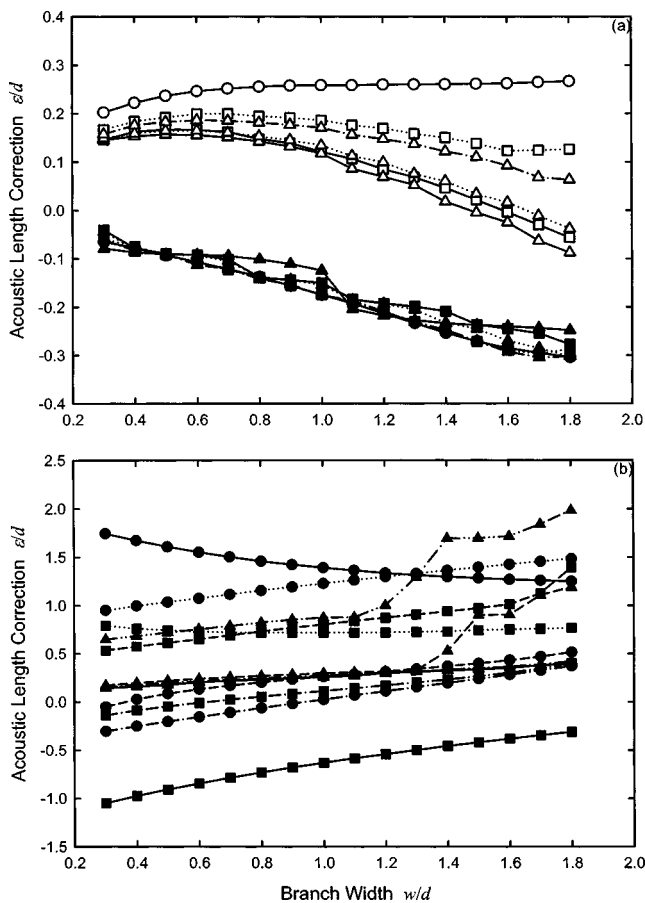


FIG. 11. Acoustic length corrections for opened sidebranches. (a) Branch length correction; (b) length correction of upstream duct section.  $\bullet$ :  $l/d = 1$ ;  $\blacksquare$ :  $l/d = 3$ ;  $\blacktriangle$ :  $l/d = 5$ . —: first order;  $\cdots$ : second order;  $-\cdot-\cdot-$ : third order;  $- - -$ : fourth order;  $-\cdot-\cdot-$ : fifth order. Closed symbols: weak impedance; open symbols: strong impedance.

“one-end-opened-one-end-closed” branch resonance. In the former case, the strong reflection takes place before the wave goes into the Tee-junction, resulting in a negative length correction. The opposite occurs in the latter cases. Examples of such resonance can be found in Figs. 9(a) and (c). For this branch length, the length corrections increase with  $w$  except for that of the second order resonance, which shows a fairly constant correction regardless of the value of  $w$ .

The very good correlation between the magnitudes of  $Z_b$  and  $Z_{in}$  for  $l/d = 5$  shown in Fig. 10 suggests that the corresponding duct resonance is mainly controlled by the “both-end-opened” branch resonance, the first one of which occurs at  $kd \sim 0.2\pi$ . Similar to the case of an infinitely long branch, the length corrections for the first three resonance are very close to each other regardless of the branch width, and all corrections are positive. The magnitudes of the corrections of the first three resonance are also comparable to those of the infinitely long branches (Fig. 6). Those of the fourth resonance appear close to those of the first three resonance until the higher branch mode is excited. As discussed before, the higher asymmetric branch mode helps the spreading of acoustical energy across the junction, resulting in a more rapidly increase in the length correction with branch width. Fifth order resonance is observed in this case. Early rapid rise in the length correction is observed. This is consistent

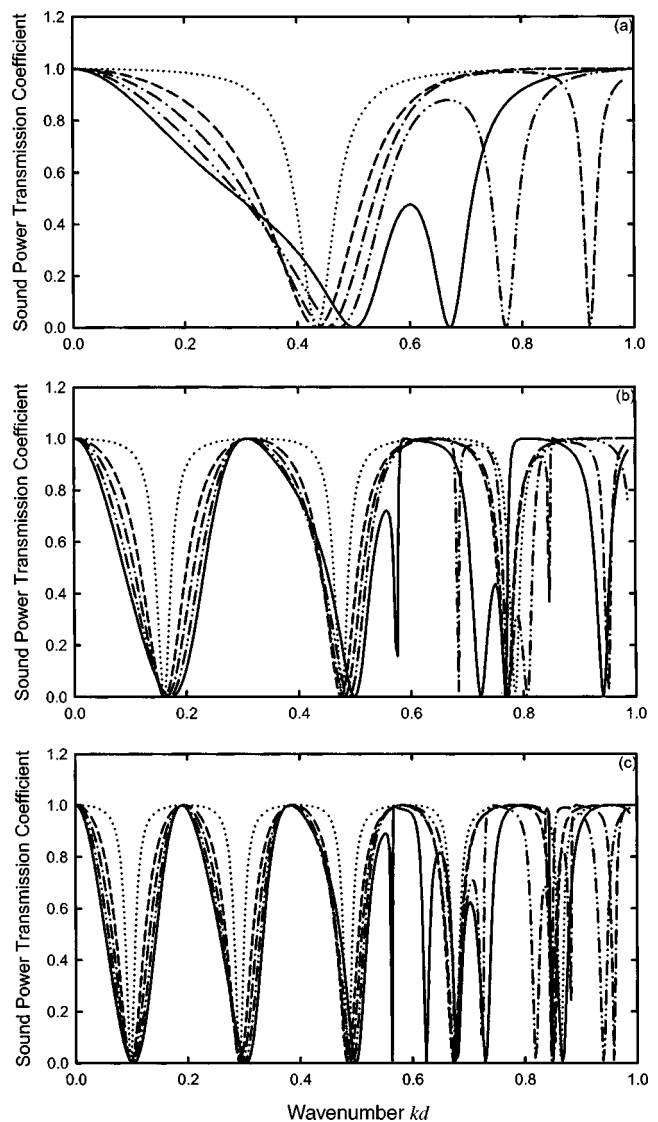


FIG. 12. Sound power transmission across closed sidebranches.  $l/d =$  (a) 1; (b) 3; (c) 5.  $\cdots$ :  $w/d = 0.3$ ;  $- - -$ :  $w/d = 0.9$ ;  $-\cdot-\cdot-$ :  $w/d = 1.2$ ;  $-\cdot-\cdot-$ :  $w/d = 1.5$ ;  $—$ :  $w/d = 1.8$ .

with the results for the infinitely long branch. In fact, a similar rapid rise in length correction can also be found in the fourth order resonance of the  $l/d = 3$  case. Results shown in Fig. 11(b) suggest that the duct length corrections can be comparable to  $d$ , implying that the conjecture of Tang and Li<sup>6</sup> on large branch separation correction is possible.

### C. Closed branches

The closed branches produce a low-pass filtering effect in sound propagation such that  $\tau \rightarrow 1$  as  $kd \rightarrow 0$ . Two types of branch resonance will occur. The first one is the “both-end-closed” one where high pressure is created in the junction. The second one is again of the “one-end-closed-one-end-opened” type but this time the low-pressure region is found inside the junction.

Figures 12(a), (b), and (c) illustrate the frequency variations of the sound power transmission coefficients for  $l/d = 1, 3$ , and  $5$ , respectively, at various  $w$ . While the wave number at the second vanishing sound transmission de-



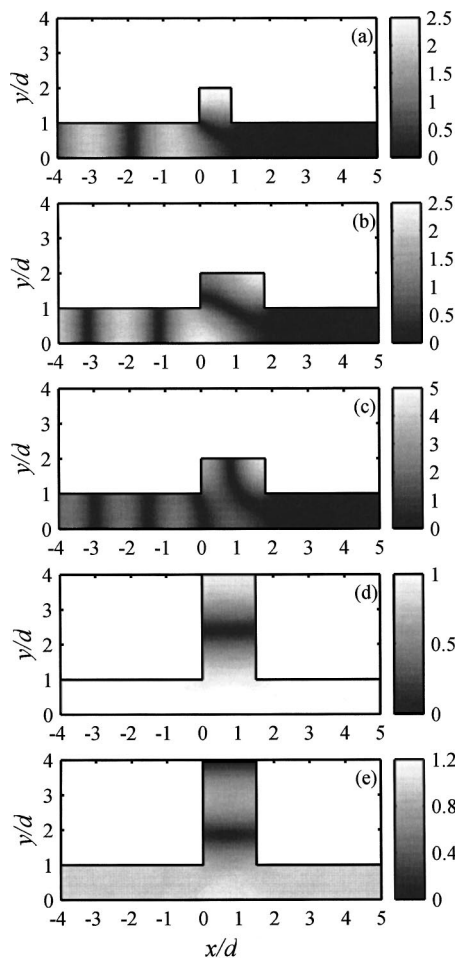


FIG. 13. Some typical examples of resonance inside the closed side-branches. (a)  $kd=0.433\pi$ ,  $w/d=0.9$ ,  $l/d=1$ ; (b)  $kd=0.500\pi$ ,  $w/d=1.8$ ;  $l/d=1$ ; (c)  $kd=0.672\pi$ ,  $w/d=1.8$ ;  $l/d=1$ ; (d)  $kd=0.312\pi$ ,  $w/d=1.5$ ;  $l/d=3$ ; (e)  $kd=0.649\pi$ ,  $w/d=1.5$ ;  $l/d=3$ .

creases with increasing  $w$  as in the opened-branch cases, that of the first one increases as  $w$  increases as shown in Fig. 12. Again the first vanishing sound transmission is due to a planar longitudinal branch resonance, but this time this resonance results in high acoustic pressure magnitude at the closed-branch end and a low acoustic pressure region inside the Tee-junction [Fig. 13(a)]. This resonance resembles that of the “one-end-closed-one-end-opened” tube. As  $w$  increases, it is more difficult to sustain a planar standing wave form inside the branch, as illustrated in Fig. 13(b), as the boundary condition at branch end in this case does not enforce uniform pressure there. The branch length for the resonance decreases as  $w$  increases, resulting in a shift of the first vanishing sound transmission  $kd$  toward the higher side. The nodal plane eventually intersects with the branch end and it is then obvious that the excitation of the first asymmetric standing branch mode soon follows, resulting in an earlier occurrence of the second vanishing sound transmission at lower  $kd$  [Fig. 13(c)].

As the branch length increases, more branch resonance occurs at lower  $kd$  as in the opened branch cases [Figs. 12(b) and (c)]. The longer the branch, the larger the number of plane wave resonances inside the branch before the excitation of the higher-standing branch modes. The patterns of  $\tau$

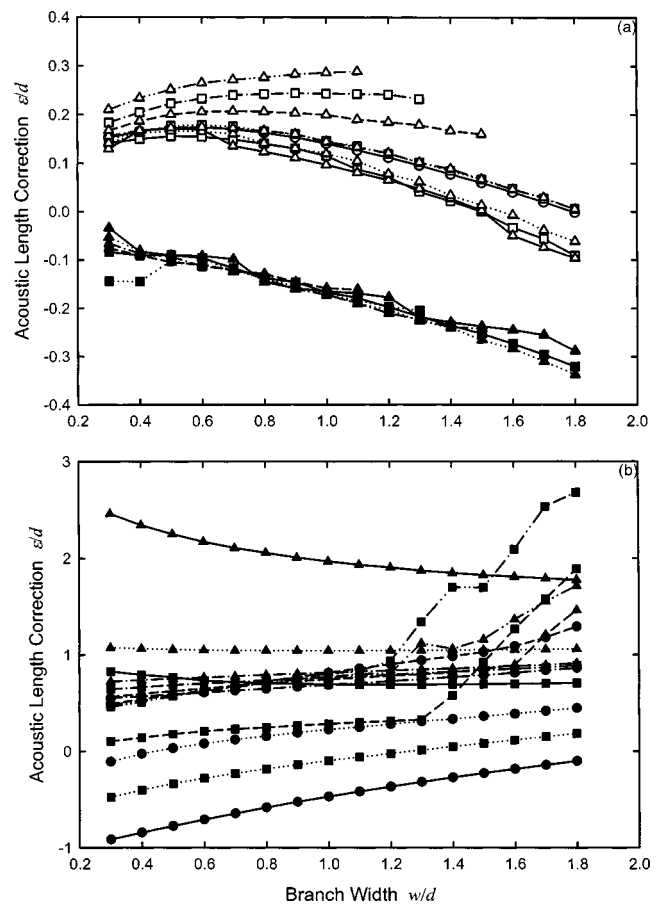


FIG. 14. Acoustic length corrections for closed sidebranches. (a) Branch length correction; (b) length correction of upstream duct section. Legends: same as those of Fig. 11.

variations in the range  $0.5\pi < kd < 0.6\pi$  for  $w/d=1.8$ ,  $l/d=3$ , in the range  $0.8\pi < kd < 0.9\pi$  for  $w/d=1.5$ ,  $l/d=3$  [Fig. 12(b)] and in similar ranges for the  $l/d=5$  cases [Fig. 12(c)] and some others are due to the same mechanism as described for the  $l/d=1$  cases [Figs. 13(a)–(c)]. Thus, the corresponding results are not discussed further.

Comparing the results shown in Figs. 7 and 12, one can find that the frequencies for the vanishing sound transmission due to the longitudinal plane wave branch resonance for the opened-branch cases correspond approximately to those of ideal sound transmission for the closed-branch cases, and vice versa. However, in the closed-branch cases, the strong and vanishing transmissions are due to a “both-ends-closed” type and a “one-end-closed-one-end-opened” type branch resonance, respectively. Some examples of the corresponding sound fields are given in Figs. 13(a), (d), and (e). The large accumulation of acoustical energy on the main duct wall immediately opposite the branch entry illustrated in Figs. 13(d) and (e) tends to suggest a relatively large branch length correction.

Figure 14(a) summarizes the branch length corrections for the first few closed-branch resonances. The observations are similar to those for the opened sidebranches [Fig. 11(a)]. The corrections correspond to the strong sound transmission cases, this time due to the “both-end-closed” type branch resonance, are negative and are not sensitive to the order of resonance and the branch length before the higher branch

modes are excited. Their values are also comparable to those of the opened-branch cases. The corrections associated with the vanishing sound transmission, resulted from the “one-end-closed-one-end-opened” type branch resonance, increase with the order of resonance, but unlike the case of the opened sidebranch, they increase with branch length. The data obtained after the excitation of higher branch modes are again excluded.

Figure 14(b) illustrates the length corrections in the main duct upstream section. Again, these resonance correspond to weak input impedance and are very often associated with the “one-end-closed-one-end-opened” branch resonance. The branch resonance is even more important when the first asymmetric branch mode is excited as it forces a weak pressure in the middle of the junction, causing strong upstream reflection [for instance, see Fig. 13(b)]. One can expect that the branch resonance takes place at frequencies earlier than those in the opened branch cases. For  $l/d=1$ , negative corrections are observed for the first order resonance over the range of  $w$  investigated. Then the corrections increase monotonically with the order of resonance. Excitation of higher branch modes is illustrated by the results of the fourth order resonance. The corrections increase with  $w$ , but show a tendency to converge before they are affected by the higher branch modes.

The situations at  $l/d=3$  resemble very much those in the opened-branch case, although the variations of the corrections with the order of resonance are opposite. In this case, the corrections due to the odd order resonance are positive and the others negative. Together with the results for the opened branches, one can conclude that the correction is negative and positive whenever a high- and low-pressure region is enforced by the branch resonance respectively. Rapid increase in the corrections can be observed again after the excitation of the higher branch modes. The duct resonance is again controlled by the vanishing sound transmission branch resonance when  $l/d=5$  (not shown here). However, before the occurrence of the higher branch mode resonance, the associated corrections decrease with some degrees of convergence as the order of resonance increases. The positive corrections are expected as the branch resonance this time tends to force a low-pressure region within the junction. One can again observe the rapid rise in the length corrections after the higher branch modes are excited.

#### IV. CONCLUSIONS

In the present study, the sound transmission characteristics of and the acoustic length corrections due to a Tee-junction along an infinitely long duct are investigated numerically using the method of finite elements. The sidebranches considered here are the infinitely long branches, and opened and closed branches. The frequency range of the present study is up to the first eigenfrequency of the main duct.

For infinitely long sidebranches, a sharp drop in the sound transmission coefficient is found at a frequency slightly higher than the first asymmetric branch eigenfrequency. The increase of the sound transmission effectiveness resumes afterward. The relatively uniform particle velocity

fields at the entry of the sidebranches at the higher branch mode eigenfrequencies delay such higher-mode excitations. The corresponding acoustic length corrections of the upstream duct section increase with branch width and the order of the resonance.

Opened sidebranches produce alternate strong and weak sound transmissions due to the occurrence of the planar branch mode resonance. At strong sound transmission, the branch length corrections are negative and their magnitudes increase as the branch width increases. They do not really depend on the order of the branch resonance. For the other planar branch resonance cases, the corrections show a slight increase with short branch width and then decrease as the branch width increases beyond that of the main duct, except for the first order resonance, which appears to stay at a particular value as the branch width increases. They also decrease with branch length and the order of the resonance. The length corrections related to the main duct do not show a very general trend, but the magnitudes of the corrections show a tendency to converge at increased branch width before the nonplanar branch modes are excited. After the excitation of such modes, the corrections increase rapidly and keep on increasing as the branch width increases.

The closed sidebranches produce actions similar to that of an expansion chamber before the nonplanar higher branch modes are excited. The excitation of the nonplanar higher branch modes reduces the sound transmission coefficients. The branch length corrections due to the strong sound transmission branch resonance are negative and the values are comparable to those of the opened-sidebranch cases. The corresponding length corrections at vanishing sound transmission increase with branch length and the order of resonance. The duct length corrections show features that are in general opposite to those observed in the opened-sidebranch cases. However, their magnitudes still show some degrees of convergence at increased branch width unless a nonplanar higher branch mode is excited. These excitations result in rapid increases in the correction magnitudes.

#### ACKNOWLEDGMENT

This work is supported by a grant from the Research Committee, The Hong Kong Polytechnic University (Project No. G-YD59).

<sup>1</sup>L. E. Kinsler, A. R. Frey, A. B. Coppens, and J. V. Sanders, *Fundamentals of Acoustics*, 4th ed. (Wiley, New York, 2000).

<sup>2</sup>D. D. Reynolds and J. M. Bledsoe, *Algorithms for HVAC Acoustics* (American Society of Heating, Refrigeration and Air-Conditioning Engineers, Atlanta, Georgia, 1991).

<sup>3</sup>J. W. Miles, “Diffraction of sound due to right angled joints in rectangular ducts,” *J. Acoust. Soc. Am.* **19**, 572–579 (1947).

<sup>4</sup>J. C. Bruggeman, “The propagation of low-frequency sound in a two-dimensional duct system with T joints and right angle bends: Theory and experiment,” *J. Acoust. Soc. Am.* **82**, 1045–1051 (1987).

<sup>5</sup>T. C. Redmore and K. A. Mulholland, “The application of mode coupling theory to the transmission of sound in the sidebranch of a rectangular duct system,” *J. Sound Vib.* **85**, 323–331 (1982).

<sup>6</sup>S. K. Tang and F. Y. C. Li, “On low frequency sound transmission loss of

double side-branches: a comparison between theory and experiment,” J. Acoust. Soc. Am. **113**, 3215–3225 (2003).

<sup>7</sup>S. K. Tang and C. K. Lau, “Sound transmission across a smooth nonuniform section in an infinitely long duct,” J. Acoust. Soc. Am. **112**, 2602–2611 (2002).

<sup>8</sup>P. M. Radavich and A. Selamet, “A computational approach for flow-acoustics coupling in closed side branches,” J. Acoust. Soc. Am. **109**, 1343–1353 (2001).

<sup>9</sup>P. M. Morse and K. U. Ingard, *Theoretical Acoustics* (McGraw-Hill, New York, 1962).